Mechanical Systems and Signal Processing 135 (2020) 106368

Contents lists available at ScienceDirect

Mechanical Systems and Signal Processing

journal homepage: www.elsevier.com/locate/ymssp

A force reflection robust control scheme with online authority adjustment for dual user haptic system

Mohammad Motaharifar, Hamid D. Taghirad *

Advanced Robotics and Automated Systems (ARAS), Industrial Control Center of Excellence, Faculty of Electrical Engineering, K. N. Toosi University of Technology, Tehran 1969764499, Iran

ARTICLE INFO

Article history:
Received 28 April 2019
Received in revised form 25 July 2019
Accepted 10 September 2019

Keywords:
Dual-user haptics
Surgery training
Robust control
Input-to-state stability (ISS)

ABSTRACT

This article aims at developing a control structure with online authority adjustment for a dual-user haptic training system. In the considered system, the trainer and the trainee are given the facility to cooperatively conduct the surgical operation. The task dominance is automatically adjusted based on the task performance of the trainee with respect to the trainer. To that effect, the average norm of position error between the trainer and the trainee is calculated in a sliding window and the relative task dominance is assigned to the operators accordingly. Moreover, a robust controller is developed to satisfy the requirement of position tracking. The stability analysis based on the input-to-state stability (ISS) methodology is reported. Experimental results demonstrate the effectiveness of the proposed control approach.

1. Introduction

Over the past several years, various aspects of medical field have rapidly developed toward more advanced conditions [1–4]. However, surgery training which is still based on direct supervision of an expert surgeon have been hardly successful to keep up with them in such advancement process. As an illustration, traditional methods of surgery training are not reliable enough owing to the limitation in active intervention of the expert surgeon during the operation. This may lead to undesired complications for the patient due to the lack of trainee's surgical skills [5]. For instance, a study on ophthalmic residents has shown that the rate of complications such as retinal lesions and amount of retinal detachment is higher for the residents with less skills [6]. For this reason, utilization of a more systematic approach to facilitate the active intervention of expert surgeons during the operation conducting by a trainee may highly reduce the rate of such complications for the patients. Thus, development of the required technology to facilitate the collaboration of a trainer and a trainee may be considered as a valuable training asset to reduce the undesired complications of surgery training.

On the other hand, the technologies derived from telerobotic and haptic systems have facilitated many aspects of surgical tasks from the training simulators [7] to the tele-operative surgeries [8–10]. A relatively emerging and relevant research field is dual user haptic systems in which the trainer and the trainee are able to collaboratively perform a certain task through their haptic devices. Facilitating the collaboration between the trainer and the trainee, the dual user haptic system has arisen as a feasible surgical training framework [11].

* Corresponding author.
E-mail addresses: motaharifar@email.kntu.ac.ir (M. Motaharifar), taghirad@kntu.ac.ir (H.D. Taghirad).

https://doi.org/10.1016/j.ymssp.2019.106368

Nomenclature

B_e	Damping of the environment
B_{hi}	Damping of the operator #i
$C_i(q_i, \dot{q}_i)$	Centripetal and Coriolis matrix of the haptic device #i
$G_i(q_i)$	Gravity vector of the haptic device #i
$J_i(q_i)$	Jacobian matrix of the haptic device #i
K_e	Stiffness of the environment
K_{hi}	Stiffness of the operator #i
K_i	Positive definite gain matrix
$M_i(q_i)$	Mass of the haptic device #i
M_{hi}	Mass of the operator #i
P_i	Response of the Lyapunov equation $\Lambda_i^T P_i + P_i \Lambda_i = -\Omega_i$
Y_i	Regressor matrix
f_i^*	exogenous force exerted by the operator #i
f_{hi}	Forces applied by the operator #i
f_{pi}	Passive part of the force applied to haptic device #i
k_i	Diagonal elements of K_i supposed to be equal
q_i	Joint position of the haptic device #i
r_i	Sliding variable
u_i	Control torque of the haptic device #i
x_i	Position of the haptic device #i
x_{di}	Desired position of the haptic device #i
Λ_i	Positive definite gain matrix
Ω_i	A positive definite matrix used as design parameter
α	Dominance factor
η_i	$Y_i^T r_i$
$\hat{\theta}_i$	The estimation of θ_i
λ_i	Diagonal elements of Λ_i supposed to be equal
ν_i	A design parameter used in the stability analysis
ω_i	Diagonal elements of Ω_i supposed to be equal
θ_i	The vector of physical parameters for the haptic device #i
θ_i^*	The nominal value of θ_i
$\tilde{\theta}_i$	Difference between θ_i and θ_i^*
ξ_i	Upper bound of the norm of $\tilde{\theta}_i$

The control design objective for dual user haptic systems is to ensure the robust stability of the system with appropriate performance. Up to now, several control schemes have been developed for dual user haptic systems to realize the mentioned objective. In order to determine the task authority of each operator, the concept of *dominance factor* has been introduced by Nudehi [12]. The concept of dominance factor has been utilized in several investigations to design various control schemes such as six-channel architecture [13], $PD + d$ control [14], adaptive control [15], etc. Although those methodologies have investigated fundamental issues of general dual user haptic systems, they have not addressed some key points regarding the surgical or training aspect of cooperation. As a case in point, the task authority is fixed during the operation in those investigations [12–15]. Nevertheless, the adjustment of task authority during the operation based on the real-time performance of the trainee is of high importance in dual user training systems. In this technique, the full/partial authority of performing the surgical operation is given to the trainee as long as his/her task performance is satisfactory. In the case that any mistake made by the trainee, the task authority is transformed to the trainer to avoid undesired complications. The control design problem for dual user haptic systems with online authority adjustment have been only considered by a few studies [16–18]. However, none of the previous works have considered real time adjustment of task authority and nonlinear stability analysis together which is the subject of this paper.

Based on the above given motivation, the main contribution of this study is design and stability analysis of a robust control scheme for dual user haptic training system with real-time authority adjustment. In contrast with the existing investigations that typically address online authority adjustment for linear dual user training systems [16–18], the presented scheme is applicable to a wider class of dual user haptic systems, namely the nonlinear dual user haptic systems with uncertainty. Furthermore, utilization of the moving average of position error as an alternative to its instantaneous value leads to more smooth behavior. In the presented framework, the trainee is allowed to perform the surgical tasks and the haptic cues from the trainer are applied as needed. For this purpose, the moving average of the position error between the trainer and the trainee is considered as a parameter to adjust the task authority in real-time. Note that, such adjustment of the task authority results to more emphasis on the long-term position errors rather than sudden mistakes. In this way, the trainee has the opportunity to correct his/her sudden mistakes in a limited time period for increased independence. Later, if the trainee is not still in the right position, the haptic feedback is implemented for long-term trends of position error. On the other hand, dynamic uncertainty is an important obstacle for the development of high performance controller for mechanical systems [19–22]. Thus, a robust control scheme is developed to ensure the position tracking of haptic devices in the presence of dynamic uncertainty. The stability of each nonlinear haptic device by applying the proposed control law is analyzed using input-to-state stability (ISS) approach, and the stability of the overall system is studied by using the small gain theorem. Note that, the linear control schemes [16–18] are able to stabilize the system only in a region in which the linear model of the system is valid. In contrast, the nonlinear nature of the proposed control structure makes it possible to guarantee the stability of closed loop system in all of its workspace.

The remainder of this article is organized as follows. Section 2 presents a brief description of the dual user haptic system. The dynamic relations of dual user haptic systems is expressed in Section 3. Our proposed control methodology is described in Section 4. The stability of nonlinear system is analyzed in Section 5. Experimental results are presented in Section 6. Finally, Section 7 gives the conclusions.

2. System description

In a dual user haptic system for surgical training application, the operation is collaboratively performed by two operators including a trainer and a trainee. The block diagram of this system is depicted in Fig. 1. The system is composed of five components: the trainer, the trainee, the haptic consoles #1, the haptic console #2, and the virtual environment. It is supposed that the virtual environment is located in a workstation at the trainee's side. Indeed, the force of virtual environment is a function of the trainee's position. The dominance of each user over the task is determined by dominance factor which is denoted by α. As depicted in the figure, the desired position of each haptic console is a weighted sum of the two positions with weights α and $1-\alpha$. The following three cases may be considered to set the value of the dominance factor:

- Dominance factor is zero; i.e., $\alpha = 0$: In this case, the task dominance is fully transformed to the trainee, and the trainer receives the position of the trainee for the evaluation purpose. Thus, the trainee is given the opportunity to freely experience the sense of surgical operation without any corrective feedback from the trainer.
- Dominance factor is unity; i.e., $\alpha = 1$: Dual to the previous case, this case corresponds to the full dominance of the trainer. Therefore, without any influence on the environment, the trainee is able to learn the skills through obtaining the position of the trainer.
- Dominance factor is between zero and unity; i.e., $0 < \alpha < 1$: In this case, both operators have partial control over the task. Thus, the trainer and the trainee collaboratively perform the operations.

To make the training more efficient, the value of dominance factor is adjusted during the operation based on the trainee's performance in performing the operations. To that effect, the normalized moving average of the position error between the trainer and the trainee is calculated and the required justifications are applied to the dominance factor accordingly. Notably, the proposed scheme is based on a special training philosophy in which the trainee is given the opportunity to freely manipulate the environment when $\alpha = 0$ and receives the haptic feedback cues from the trainer when $\alpha = 1$ as the position error between the trainer and trainee grows. Indeed, through the proposed surgery training structure, the trainee is allowed to learn the surgical skills by performing the surgery and receiving haptic feedback from the trainer and the environment. The dominance factor is adjusted such that the trainee is given the facility to progressively conduct the task independently during the training procedure. Toward this end, the haptic feedback to the trainee's hands is applied only for the long-term trends and not the short term fluctuations of position error. This gives the trainee the opportunity to correct his/her wrong

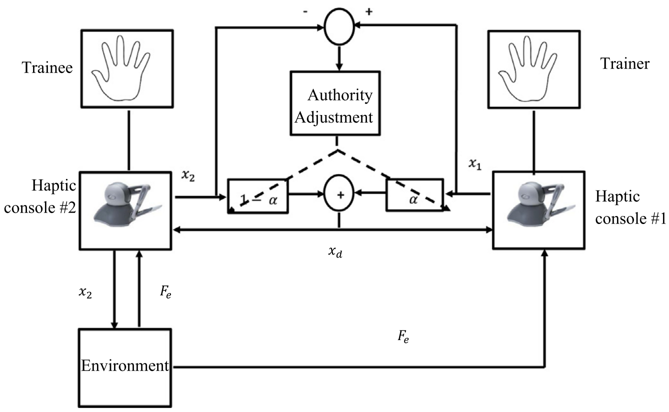

Fig. 1. The haptic system for surgery training.

motion in a limited time period. Then, in the case that the trainee is not still in the correct path up to some time, the haptic feedback is applied to guide the trainee to the right position. The mathematical relations of the proposed scheme will be elaborated later.

3. System dynamics

The dynamics of each haptic device in a dual user haptic training system is expressed as [23]

$$M_i(q_i)\ddot{q}_i + C_i(q_i,\dot{q}_i)\dot{q}_i + G_i(q_i) = u_i + J_i^T(q_i)f_{hi} \quad (1)$$

where $q_i \in \mathbb{R}^{n\times1}$ is the joint position vector, and $M_i(q_i) \in \mathbb{R}^{n\times n}, C_i(q_i,\dot{q}_i)\dot{q}_i \in \mathbb{R}^{n\times n}$, and $G_i(q_i) \in \mathbb{R}^{n\times1}$ denote the mass matrices, the centripetal and Coriolis matrices, and the gravity vectors, respectively. Besides, $u_i \in \mathbb{R}^{n\times1}$ denote the control torque vectors, and $f_{hi} \in \mathbb{R}^{n\times1}$ are the forces applied by the operators. Throughout this paper, the subscript i represents the haptic console #1 for $i = 1$ and haptic console # 2 for $i = 2$.

Next, some useful properties of the dynamic Eq. (1) are presented.

Property 1. *The mass matrix $M_i(q_i)$ is symmetric and positive definite.*

Property 2. *The matrix $\dot{M}_i(q_i) - 2C(q_i,\dot{q}_i)$ is skew symmetric; that is,*

$$x^T\left(\dot{M}_i(q_i) - 2C_i(q_i,\dot{q}_i)\right)x = 0 \quad \forall x \in \mathbb{R}^n.$$

Property 3. *The left hand side of the dynamic models is linear in a set of physical parameters as follows:*

$$M_i(q_i)\ddot{q}_i + C_i(q_i,\dot{q}_i)\dot{q}_i + G_i(q_i) = Y_i(q_i,\dot{q}_i,\ddot{q}_i)\theta_i \quad (2)$$

where $Y_i(\cdot)$ is called the regressor and θ_i is the vector of physical parameters.

Furthermore, the forward kinematic relation for obtaining the position vector of end effector denoted by $x_i \in \mathbb{R}^{n\times1}$ is presented as ([24])

$$x_i = k_i(q_i) \quad (3)$$

where $k_i(\cdot)$ is a nonlinear function. In addition, the relation between the velocity vectors in joint space and task space is stated as

$$\dot{x}_i = J_i(q_i)\dot{q}_i \quad (4)$$

where $J_i(q_i)$ is the Jacobian matrix. Next, both sides of (4) are differentiated with respect to time to obtain the acceleration in task space as

$$\ddot{x}_i = J_i(q_i)\ddot{q}_i + \dot{J}_i(q_i)\dot{q}_i. \quad (5)$$

The forces applied by the environment and the operators' hands are presumed to satisfy some assumptions as presented in below.

Assumption 1. The surgical tool is assumed to be in contact with the virtual environment at the trainee side. Thus, the environment force is a function of the trainee's position defined as

$$f_e = -B_e\dot{x}_2 - K_e x_2 \quad (6)$$

Assumption 2. The hand forces applied by human operators are assumed as [25,26]

$$f_{hi} = f_{hi}^* - M_{hi}\ddot{x}_i - B_{hi}\dot{x}_i - K_{hi}x_i \quad (7)$$

where f_i^* is the exogenous force exerted by the operator #i and M_{hi}, B_{hi}, and K_{hi} are constant, symmetric, and positive definite matrices corresponding to the mass, damping, and stiffness of the operator #i, respectively. Note that, the formulation given in (7) is composed of both passive and active components. Indeed, the terms involving either the mass, the damping, or the stiffness of the operator indicate the passive reaction of the operator's hand to the motion of haptic device, whereas exogenous force input is an active component that is voluntary produced by the operator to move the haptic device toward the desired position.

4. The proposed control methodology

As already explained, the proposed control methodology utilizes dominance factor to specify the dominance of each operator over the task. It is assumed that the trainee have enough expertise to conduct the operation with the trainer's supervision. Therefore, the initial value of the dominance factor is set as unity to give the full authority to the trainee. Then, the value of the dominance factor is adjusted during the operations based on the trainee's performance. In order to assess the trainee's performance, the normalized value of position error between the trainer and the trainee is utilized. Besides, in order that the sudden and short-time variations of the error do not unwantedly affect the dominance factor, the moving average of position error is utilized. In fact, using the moving average generally leads to more emphasis on the longer term trends rather than the sudden and short-time fluctuations. Furthermore, a dead-zone function is used to avoid the change of dominance factor due to small values of position error. This also gives the trainee some freedom in performing the procedures. As a result, the dominance factor is mathematically formulated as

$$\alpha = 1 - \psi\left(\frac{1}{t_w x_n}\int_{t-t_w}^{t} \|x_1 - x_2\| dt\right) \tag{8}$$

where x_1 and x_2 are the positions of the trainer and the trainee haptic devices, t_w is the window size of moving average, and x_n is the normalization parameter. In this paper, the worst-case norm of position error is utilized as the normalization parameter. Moreover, $\psi(.)$ is any function that provides smooth transition between 0 and 1. An example of such function may be considered as

$$\psi(\chi) = 1 - \sum_{i=0}^{N} \frac{\sigma^i \chi^i}{i!} e^{-\sigma\chi}$$

where the positive integer number N and the positive real number σ are two design parameters that determine sharpness of transition. As an example, this function is depicted in Fig. 2 for $N = 10$ and $\sigma = 500$.

Then, the desired task space positions of the haptic devices are presented as

$$x_{d1} = x_{d2} = \alpha x_1 + (1-\alpha) x_2 \tag{9}$$

The above relation shows that if $\alpha = 0$, the current position of trainee is the desired position of both haptic consoles. Thus, the trainer's haptic console tracks the position of the trainee and the trainer receives the position information of the surgical tool. On the other hand, the desired position of the trainee haptic console in the trainee dominant mode is the trainee haptic console itself. This means that the position error of trainee haptic console is zero and the trainee is able to freely conduct the surgical operation without any interference by the haptic system.

Next, a control scheme is developed for each haptic device such that the reference position x_d is tracked. To that effect, the control law is defined as

$$u_i = \widehat{M}_i(q_i)\dot{v}_i + \widehat{C}_i(q_i,\dot{q}_i)v_i + \widehat{G}_i(q_i) - K_i r_i + J_i^T(q_i) f_e \tag{10}$$

where $K_i \in \mathbb{R}^{n\times n}$ is a positive definite matrix and the notation $\hat{(\cdot)}$ denotes the estimated value of $(\cdot)$ that will be elaborated later. In addition,

$$v_i = J_i^{-1}(q_i)\Lambda_i \tilde{x}_i r_i = \dot{q}_i - v_i \tag{11}$$

where $\tilde{x}_i = x_d - x_i$ and $\Lambda_i \in \mathbb{R}^{n\times n}$ is a positive definite matrix. Using Property 3, the control law (10) is represented as

$$u_i = Y_i\hat{\theta}_i - K_i r_i + J_i^T(q_i) f_e \tag{12}$$

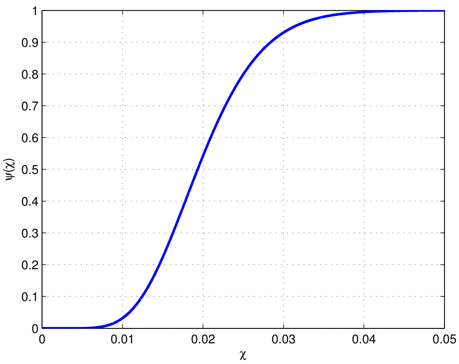

Fig. 2. The transition function $\psi(\chi)$.

Furthermore, the control law (12) is combined with the dynamical Eq. (1) to obtain the closed loop dynamic equation as

$$M_i(q_i)\dot{r}_i + C_i(q_i,\dot{q}_i)r_i + K_i r_i = Y_i\left(\hat{\theta}_i - \theta_i\right) + J_i^T(q_i)f_{hi} + J_i^T(q_i)f_e \tag{13}$$

in which the term $\hat{\theta}_i$ in (12) is chosen as

$$\hat{\theta}_i = \theta_i^* + \delta\theta_i \tag{14}$$

where θ_i^* is the nominal value of θ_i and $\delta\theta_i$ is an extra control term. Suppose that the uncertainty is bounded by a positive constant ξ_i such that

$$\|\tilde{\theta}_i\| = \|\theta_i - \theta_i^*\| \leqslant \xi_i. \tag{15}$$

Then, the extra control term $\delta\theta_i$ is selected as [23]

$$\delta\theta_i = \begin{cases} -\xi_i \frac{Y_i^T r_i}{\|Y_i^T r_i\|}, & \|Y_i^T r_i\| > \mu_i \\ -\frac{\xi_i}{\mu_i} Y_i^T r_i, & \|Y_i^T r_i\| \leqslant \mu_i \end{cases} \tag{16}$$

where the design parameter μ_i is a small positive value.

5. Stability analysis

In this section, the stability of the proposed control structure for dual user haptic system is investigated using the ISS methodology and the small gain theorem. The approach is to analyze the stability of each haptic device using the ISS and to use the small gain theorem for the stability of the overall system. First, the definition of ISS is presented.

Definition 1. (ISS Stability) ([27], p. 175): The dynamic system in the general form of

$$\dot{x} = f(t,x,u) \tag{17}$$

where $f : [0,\infty) \times \mathbb{R}^n \times \mathbb{R}^m \to \mathbb{R}^n$ is a piecewise continuous function in t and locally Lipschitz in x and u. The system (17) is ISS if a class $\mathcal{KL}$ function β and a class $\mathcal{K}$ function γ exist such that for any initial condition x_0 and any bounded input the inequality

$$\|x(t)\| \leqslant \beta(\|x_0\|,t) + \gamma(\sup\|u_T(t)\|), \qquad 0 \leqslant t \leqslant T \tag{18}$$

is satisfied.

Next, a connection between the concept of the presented definition of ISS and the Lyapunov theory is presented in the following theorem:

Theorem 1. (ISS Stability Theorem) [27], p. 176: *Let there exists a continuously differentiable Lyapunov candidate function* $V : [0,\infty) \times \mathbb{R}^n \to \mathbb{R}$ *such that*

$$\begin{aligned} &\alpha_1(\|x\|) \leqslant V(x) \leqslant \alpha_2(\|x\|) \\ &\dot{V}(x) \leqslant -W(x), \qquad \forall \|x\| \geqslant \rho(\|u\|) > 0 \end{aligned}$$

where $\dot{V}$ is the derivative of the Lyapunov candidate function along the solutions of the system (17), α_1 and α_2 are class $\mathcal{K}_\infty$ functions, ρ is class $\mathcal{K}$ function, and $W(x)$ is a positive definite function on $\mathbb{R}^n$. Then, the system (17) is ISS with gain $\gamma = \alpha_1^{-1} \circ \alpha_2 \circ \rho$ where the operator $\circ$ denotes the function composition opertion.

At the next lemma, the quadratic inequality known as the Young's inequality is presented.

Lemma 1. (Young's Inequality) [28]: *Suppose that x and y are arbitrary vectors and ϵ is a positive scalar. Then, the following inequality is satisfied:*

$$|x^T y| \leqslant \left(\frac{\epsilon}{2}\right)\|x\|^2 + \left(\frac{1}{2\epsilon}\right)\|y\|^2. \tag{19}$$

Next, a unique formulation is stated to analyze the stability of the two haptic devices. This unique formulation is later utilized to investigate the stability of each haptic device. To obtain such unique formulation, the closed loop system (13) is combined with the relations for environment force and force of human operators presented in (6) and (7), respectively to obtain

$$M_i(q_i)\dot{r}_i + C_i(q_i,\dot{q}_i)r_i + K_i r_i = Y_i\left(\hat{\theta}_i - \theta_i\right) + J_i^T(q_i)f_{xi} + J_i^T(q_i)f_{pi} \tag{20}$$

where f_{xi} is the exogenous part of the force, while f_{pi} is the passive part of the force defined as

$$f_{pi} = -M_{pi}\ddot{x}_i - B_{pi}\dot{x}_i - K_{pi}x_i. \tag{21}$$

For the trainer side, the environment force is considered as an exogenous force, whereas it is included in the passive component in the trainee side. Therefore, the exogenous part of the force at the two sides are defined as

$$f_{x1} = f_e + f^*_{h1} f_{x2} = f^*_{h2} \tag{22}$$

Moreover, the parameters related to the passive part of force at the two sides are defined as

$$M_{p1} = M_{h1}, \quad M_{p2} = M_{h2}, B_{p1} = B_{h1}, \quad B_{p2} = B_{h2} + B_e, K_{p1} = K_{h1}, \quad K_{p2} = K_{h2} + K_e. \tag{23}$$

Now, the stability of the presented unique formulation for haptic devices is analyzed.

Proposition 1. *The closed loop of the haptic console #i formulated in (20) may be made ISS with respect to state $[r_i^T, \tilde{x}_i^T]^T$ and the input $\left[x_d^T, \dot{x}_d^T, f_{xi}^T, \xi_i\right]^T$.*

Proof. First, (21) is combined with (20) and (4) and (5) are used to reformulate the closed loop system as

$$\begin{aligned}
&\left(M_i(q_i) + J_i^T(q_i)M_{pi}J_i(q_i)\right)\dot{r}_i + \left(C_i(q_i,\dot{q}_i) + J_i^T(q_i)B_{pi}J_i(q_i) + J_i^T(q_i)M_{pi}\dot{J}_i(q_i)\right)r_i + \left(K_i + J_i^T(q_i)K_{pi}J_i(q_i)\right)r_i - J_i^T(q_i)B_{pi}\Lambda\tilde{x}\\
&\quad - J_i^T(q_i)M_{pi}\Lambda\dot{x} + J_i^T(q_i)M_{pi}\Lambda\dot{x}_d + J_i^T(q_i)K_{pi}\Lambda x\\
&\quad = Y_i\left(\hat{\theta}_i - \theta_i\right) + J_i^T(q_i)f_{xi}
\end{aligned} \tag{24}$$

Besides, it may be concluded from (11) that

$$\dot{\tilde{x}}_i = -\Lambda_i\tilde{x}_i + J_i^T(q_i)r_i - \dot{x}_d. \tag{25}$$

In view of the fact that $-\Lambda_i$ is a Hurwitz matrix, there always exists a unique positive definite solution P_i for the Lyapunove equation $\Lambda_i^T P_i + P_i\Lambda_i = \Omega_i$ with the positive definite matrix Ω_i. Then, a Lyapunov function candidate is considered as

$$V_i = \frac{1}{2}r_i^T\left(M_i(q_i) + J_i^T(q_i)M_{pi}J_i(q_i)\right)r_i + \epsilon_i\tilde{x}_i^T P_i\tilde{x}_i \tag{26}$$

where ϵ_i is a positive scalar. Afterwards, using Property 2 and after some manipulation, $\dot{V}_i$ is calculated along the trajectories of (24) as follows:

$$\begin{aligned}
\dot{V}_i = &-r_i^T\left(K_i + J_i^T(q_i)B_{pi}J_i(q_i)\right)r_i - \epsilon_i\tilde{x}_i\Omega_i\tilde{x}_i + 2\epsilon_i\tilde{x}_i^T P_i J_i(q_i)r_i + r_i^T J_i^T(q_i)M_{pi}\Lambda_i^2\tilde{x}_i - r_i^T J_i^T(q_i)M_{pi}\Lambda_i J_i(q_i)r_i - r_i^T J_i^T(q_i)B_{pi}\Lambda_i\tilde{x}_i\\
&+ r_i^T J_i^T(q_i)K_{pi}\tilde{x}_i - 2\epsilon_i\tilde{x}_i^T P_i\dot{x}_d + r_i^T J_i^T(q_i)M_{pi}\Lambda_i\dot{x}_d + r_i^T J_i^T(q_i)K_{pi}x_d + r_i^T Y_i\left(\tilde{\theta}_i + \delta\theta_i\right) + r_i^T J_i^T(q_i)f_{xi}
\end{aligned} \tag{27}$$

Now the following variable is defined:

$$\Xi = J_i^T(q_i)M_{pi}\Lambda_i^2 - J_i^T(q_i)B_{pi}\Lambda_i + J_i^T(q_i)K_{pi}. \tag{28}$$

On the other hand, it may be inferred from Lemma 1 that

$$\begin{aligned}
\tilde{x}_i^T\Xi r_i &\leqslant \frac{1}{8}\epsilon_i\lambda_{\min}(\Omega_i)\|\tilde{x}_i\|^2 + \frac{2\|\Xi\|^2}{\epsilon_i\lambda_{\min}(\Omega_i)}\|r_i\| - 2\epsilon_i\tilde{x}_i^T P_i\dot{x}_d \leqslant \frac{1}{8}\epsilon_i\lambda_{\min}(\Omega_i)\|\tilde{x}_i\|^2 + \frac{8\epsilon_i\|P_i\|^2}{\lambda_{\min}(\Omega_i)}\|\dot{x}_d\| r_i^T J_i^T(q_i)M_{pi}\Lambda_i\dot{x}_d\\
&\leqslant \frac{1}{8}\lambda_{\min}(K_i)\|r_i\|^2 + \frac{2J_{Mi}^2\|M_{pi}\|^2\|\Lambda_i\|^2}{\lambda_{\min}(K_i)}\|\dot{x}_d\| r_i^T J_i^T(q_i)K_{pi}x_d \leqslant \frac{1}{8}\lambda_{\min}(K_i)\|r_i\|^2 + \frac{2J_{Mi}^2\|K_{pi}\|^2}{\lambda_{\min}(K_i)}\|x_d\| r_i^T J_i^T(q_i)f_{xi}\\
&\leqslant \frac{1}{8}\lambda_{\min}(K_i)\|r_i\|^2 + \frac{2J_{Mi}^2}{\lambda_{\min}(K_i)}\|f_{xi}\|
\end{aligned} \tag{29}$$

where

$$J_{Mi} = \sup\|J_i^T(q_i)\|. \tag{30}$$

Besides, ϵ_i is selected as

$$\epsilon_i = \frac{\lambda_{\min}(K_i)\lambda_{\min}(\Omega_i)}{v_i^2\|P_i\|^2 J_{M1}^2} \tag{31}$$

where the positive value v_i is considered as a design parameter. An appropriate value of this parameter is obtained through an optimization procedure which will be explained later. Then, the following inequality is resulted:

$$-\frac{1}{v_i}r_i^T K_i r_i - \frac{1}{v_i}\epsilon_i\tilde{x}_i\Omega_i\tilde{x}_i + 2\epsilon_i\tilde{x}_i^T P_i J_i(q_i)r_i \leqslant -\left(\frac{1}{v_i}\lambda_{\min}(K_i)r_i + \frac{1}{v_i}\epsilon_i\lambda_{\min}(\Omega_i)\tilde{x}_i\right)^2 \tag{32}$$

Furthermore, by defining $\eta_i = Y_i^T r_i$ and using (15), it is concluded that

$$\eta_i^T\left(\tilde{\theta}_i + \delta\theta_i\right) \leqslant \eta_i^T\left(\xi_i \frac{\eta_i}{\|\eta_i\|} + \delta\theta_i\right) \tag{33}$$

If (16) and (33) are combined, for $\|\eta_i\| > \mu_i$ results to $\eta_1^T\left(\tilde{\theta}_1 + \delta\theta_1\right) \le 0$. In the case that $\|\eta_i\| \leqslant \mu_i$, the following relation is resulted:

$$\eta_i^T\left(\tilde{\theta}_i + \delta\theta_i\right) \leqslant \eta_i^T\left(\xi_i \frac{\eta_i}{\|\eta_i\|} - \frac{\xi_i}{\mu_i}\eta_i\right) = \xi_i\|\eta_i\| - \frac{\xi_i}{\mu_i}\|\eta_i\|^2$$

Note that, the expression $\xi_i\|\eta_1\| - \frac{\xi_i}{\mu_i}\|\eta_i\|^2$ has a maximum value $\mu_i\frac{\xi_i}{2}$ when $\|\eta_i\| = \frac{\mu_i}{2}$. Now, utilizing this fact and using (29) and (32), it may be concluded from (27) that

$$\dot{V}_i \leqslant -a_{i1}\|r_i\|^2 - a_{i2}\|\tilde{x}_i\|^2 + a_{i3}\|x_d\|^2 + a_{i4}\|\dot{x}_d\|^2 + a_{i5}\|f_{xi}\|^2 + a_{i6}\|\xi_i\| \tag{34}$$

where

$$a_{i1} = \left(\frac{5}{8} - \frac{1}{v_i}\right)\lambda_{\min}(K_i) + \lambda_{\min}\left(J_i^T(q_i)B_{pi}J_i(q_i)\right) - \frac{2\|\Xi_i\|^2}{\epsilon_i\lambda_{\min}(\Omega_i)} - \lambda_{\max}\left(J_i^T(q_i)M_{pi}\Lambda_iJ_i(q_i)\right)a_{i2} = \left(\frac{6}{8} - \frac{1}{v_i}\right)\epsilon_i\lambda_{\min}(\Omega_i)a_{i3} = \frac{2J_{Mi}^2\|K_{pi}\|^2}{\lambda_{\min}(K_i)}a_{i4} = \frac{8\epsilon_i\|P_i\|^2}{\lambda_{\min}(\Omega_i)} + \frac{2J_{Mi}^2\|M_{pi}\|^2\|\Lambda_i\|^2}{\lambda_{\min}(K_i)}a_{i5} = \frac{2J_{Mi}^2}{\lambda_{\min}(K_i)}a_{i6} = \frac{\mu_i}{2} \tag{35}$$

Now, the state vector and the input vector are selected as $\zeta_i = \left[r_i^T, \tilde{x}_i^T\right]^T$ and $\upsilon_i = \left[x_d^T, \dot{x}_d^T, f_{xi}^T, \xi_i\right]^T$. Next, an arbitrary parameter κ that satisfies $0 < \kappa < 1$ is selected. Then, it is inferred from (34) that

$$\dot{V}_i = -\kappa\min(a_{i1}, a_{i2})\|\zeta\|^2 - (1-\kappa)\min(a_{i1}, a_{i2})\|\zeta\|^2 + \max(a_{i3}, a_{i4}, a_{i5}, a_{i6})\|\upsilon\|^2 \tag{36}$$

which verifies that

$$\dot{V} \leqslant -\kappa\min(a_1, a_2)\|\zeta\|^2 \tag{37}$$

for all

$$\|\zeta\|^2 \geqslant \frac{\max(a_{i3}, a_{i4}, a_{i5}, a_{i6})}{(1-\kappa)\min(a_{i1}, a_{i2})}\|\upsilon\|^2.$$

From (26) and (37), the system can be made ISS with state ζ and the input υ, which completes the proof. □

In the next two propositions, the stability of each haptic device is concluded from Proposition 1.

Proposition 2. The haptic console #1 subsystem (13) can be made ISS with respect to the state $\left[r_1^T, \tilde{x}_1^T\right]^T$ and input $\left[x_d^T, \dot{x}_d^T, (f_{h1}^* + f_e)^T, \xi_1\right]^T$.

Proof. It can be seen that the haptic console #1 subsystem can be reformulated as (20) with $f_{x1} = f_{h1}^* + f_e$. Then, applying Proposition 1 completes the proof. □

Proposition 3. *The haptic console #2 subsystem (13) can be made ISS with respect to the state* $\left[r_2^T, \tilde{x}_2^T\right]^T$ *and input* $\left[x_d^T, \dot{x}_d^T, f_{h2}^{*T}, \xi_2\right]^T$.

Proof. Similar to the proof of Proposition 2, applying Proposition 1 on system (20) with $f_{x2} = f_{h2}^*$ completes the proof. □

Theorem 2. *Suppose that the control scheme (10) is applied to the haptic surgical training system (1). Then, the overall system can be made ISS.*

Proof. The ISS small gain approach of [29] is utilized in the stability analysis of the overall surgery training haptic system. From Proposition 2 the closed loop system of the haptic console #1 is ISS with respect to the state $\left[r_1^T, \tilde{x}_1^T\right]^T$ and input $\left[x_d^T, \dot{x}_d^T, (f_{h1}^* + f_e)^T, \xi_1\right]^T$. Consider that the ISS gain of this system is denoted by γ_1. In addition, Proposition 3 shows that the haptic console #2 subsystem is ISS with respect to the state $\left[r_2^T, \tilde{x}_2^T\right]^T$ and input $\left[x_d^T, \dot{x}_d^T, f_{h2}^{*T}, \xi_2\right]^T$. It is supposed that γ_2 is the ISS gain of the haptic console #2 subsystem. From the small gain theorem, the overall dual user haptic surgical training system is ISS if $\gamma_1\gamma_2 < 1$. □

Remark 1. From Property 1, there always exist positive scalars λ_{mi} and λ_{Mi} such that

$$\lambda_{mi} I < M_i(q_i) + J_i^T(q_i) M_{pi} J_i(q_i) < \lambda_{Mi}. \tag{38}$$

Note that, the parameters λ_{mi} and λ_{Mi} should be calculated to find the ISS gain of the system as presented in Theorem 1.

Remark 2. From (34) and (35), the condition $a_{i1} > 0$ ensures the stability of each haptic device. It is possible to hold this condition by choosing $\lambda_{\min}(K_i) > 0$ sufficiently large. Furthermore, the small gain condition $\gamma_1\gamma_2 < 1$ should be satisfied to guarantee the stability of the overall system.

Remark 3. The proposed control scheme is developed under the assumption that the trainer and the trainee are working in the vicinity of each other; thus, communication delay is not considerable. Nevertheless, the stability analysis of the overall system may be extended by considering non-negligible time delay in the communication channel. To that effect, a lemma regarding the ISS of dynamical systems subject to communication delay from [30] is utilized. In that lemma, the dynamical system $\dot{x} = F(x, u, v)$ is assumed to be ISS with respect to the state x and the input $[u, v]$. Then, the ISS of dynamical system $\dot{x} = F(x, u(t-\tau), v)$ with respect to the state x and the input $[u(t-\tau), v]$ is proven. By utilizing the explained lemma, our stability analysis may be extended to consider communication delay by verifying the ISS of each haptic console under time delay in the input channel. Afterwards, the ISS of overall system is concluded using the small gain theorem in the same way as of Theorem 2.

6. Experimental results

The experimental studies are conducted using two 3-DOF Geomagic Touch™ haptic devices as shown in Fig. 3. The controller for each haptic device is implemented on a computer and a UDP-based communication channel is harnessed to exchange data between the computers. The controller is implemented in MATLAB Simulink using a C MEX S-function and a program in C++ language using the OpenHaptics® SDK. A graphical interface is provided for each operator to observe her/his own hand position as well as the other operators' hand position. The haptic console #1 and haptic console #2 are controlled by the trainer and the trainee, respectively. As suggested by [31], in the experiments, the trainer is asked to use her/his dominant hand, while the trainee is requested to use her/his nondominant hand. Hence, the trainer has more expertise than the trainee in performing the tasks.

As for selecting the control parameters, it is necessary to hold the conditions mentioned in Remark 2 to guarantee the stability of the haptic system. In this research, a numerical analysis is followed to ensure that the stability conditions are satisfied. To that effect, the Matlab constrained optimization routine is utilized to obtain the minimum possible positive value for the ISS gain. First, the parameters of the operators hands are set to $M_{hi} = m_{hi} I$, $B_{hi} = b_{hi} I$, and $K_{hi} = k_{hi} I$ where $m_{hi} = 9\,\mathrm{g}$, $b_{hi} = 2\mathrm{N.s/m}$, and $k_{hi} = 200\mathrm{N/m}$ [13]. In order to ensure the correctness of the analysis for a wide range of operators, all of the calculations are also preformed for the hand parameters with 10% above and below the considered values. Besides, the environment force is considered as (6) where the parameters are set to $K_e = 50\mathrm{N/m}, B_e = 5\mathrm{N} \cdot s/m$. Then, the parameters J_{Mi}, λ_{mi}, and λ_{Mi} are calculated using the MATLAB function `fmincon` by considering the following ranges:

$$-\frac{\pi}{2} \leqslant q_{i1} \leqslant \frac{\pi}{2}, \quad 0 \leqslant q_{i2} \leqslant \frac{\pi}{2}, \quad 0 \leqslant q_{i3} \leqslant \frac{\pi}{2} \tag{39}$$

where q_{ij} represents position of the jth joint angle of the haptic console #i for $i = 1, 2$, $j = 1, 2, 3$. Following the procedure of finding the mentioned parameters leads to $J_{Mi} = 0.27, \lambda_{Mi} = 0.0047$, and $\lambda_{mi} = 0.0008$. Then, it is assumed that $K_1 = K_2, \Lambda_1 = \Lambda_2, K_i = k_i I_{3\times3}$, and $\Lambda_i = \lambda_i I_{3\times3}$ and the stability of the system is examined at a number of grid points in the range of $10 < k_i < 500, 10 < \lambda_i < 30$. To that effect, the Lyapunov equation $\Lambda_i^T P_i + P_i \Lambda_i = -\Omega_i$ with $\Omega_i = \omega_i I_{3\times3}$ is considered at each point and the minimum positive ISS gains are calculated for each point with ω_i and ν_i as the optimization parameters. Then, the small gain condition is examined for the calculated values of ISS gains. The condition $a_{i1} > 0$ is also examined in this procedure by penalizing the negative values of a_{i1}. Fig. 4 depicts the grid points satisfying the stability conditions in

Fig. 3. The experimental setup.

blue stars and boundary in red line. Picking up a point from the area shown by blue stars ensures that the stability conditions are satisfied. In this research, these parameters are selected as $k_i = 20$ and $\lambda_i = 20$ for $i = 1, 2$. The window size and the normalization parameter are also set as $t_w = 2s$ and $x_n = 0.5m$.

In the first part of the experiments the results obtained by implementing the proposed approach for authority adjustment and benchmark [16] that involves online authority adjustment are compared. The benchmark proposes a methodology for switching dominance factor between 0 and 1. The default value of dominance factor is 0 which is valid for the values of position error less than a predefined boundary. As soon as the position error crosses the boundary, the dominance factor immediately switches from 0 to 1 and the authority is transformed from the trainee to the trainer. Note that, the benchmark suggests abrupt change of dominance factor based on the instantaneous value of position error, while in our proposed approach the dominance factor smoothly switches based on the moving average of position error.

The results of both the benchmark [16] and the proposed approach are shown in Fig. 5. The position signals resulted from the benchmark are shown in Fig. 5a, while the position signals obtained from the proposed approach are shown in Fig. 5b. The position of the trainer's haptic device and the trainee's haptic device are depicted by solid (blue) line and dashed (red) line, respectively. In addition, the dominance factor of the benchmark and the proposed approach are shown in Fig. 5c and Fig. 5d, respectively. In both experiments, the trainee is asked to deliberately apply wrong commands for a few seconds to generate position error so as the response of the haptic system in modifying the trainee's mistakes is examined. It is evident from Fig. 5 that the position signals resulted from benchmark almost depict a fluctuating behavior at the periods of time in which position error is deliberately increased by the trainee. The primary reason of such phenomenon is the abrupt switch of dominance factor based on the instantaneous value of error. Such dependency puts to much emphasis on any variation of the position error and causes the dominance factor and the position variables to fluctuate. On the other hand, the position signals obtained from the proposed approach show more smooth and satisfactory behavior as depicted in Fig. 5. Next, the dominance factor resulted from the two approaches are compared. As depicted in Fig. 5c and Fig. 5d, the results of the benchmark and the proposed approach shows that smooth switching of dominance factor based on the moving average of the position error filters out sudden and short-term fluctuations of position error and underlines the longer-term trends. As a result, the trainee is given the opportunity to correct his/her wrong motion in a limited time period, leading to the increased independence. Moreover, by avoiding the abrupt change of dominance factor, the proposed approach shows more smooth behavior in contrast to the benchmark which depicts a fluctuating behavior in the position signals.

Furthermore, another feature of the proposed approach is studied by comparing the force signals exerted to the hands of the operators and the force of virtual environment. As already explained, through the proposed approach the trainee is given the opportunity to experience the sense of surgical operation when $\alpha = 0$ and receives the haptic feedback cues from the trainer when $\alpha = 1$ as the position error between the trainer and trainee grows. Indeed, the role of the trainee haptic console is to recreate the sense of touch for the trainee when $\alpha = 0$ and guide the trainee to the correct path when $\alpha = 1$. The force signals are depicted in Fig. 5e and Fig. 5f, for the benchmark and the proposed approach, respectively. The force signal exerted to the trainer's hand and the trainee's hand are depicted by solid (blue) line and dashed (red) line, respectively and the contact force of the environment is depicted by dashed-dotted (green) line. It is evident from the force signals of the benchmark that the sense of touch with the environment for the trainee is destroyed in most of the experiment times except when the trainee performs the operation perfectly and without error. In other words, the trainee is not given enough opportunity to freely experience the sense of operation. In contrast, the results obtained from the proposed approach show that the force of environment mostly matches the trainee's force. This means that the trainee freely experience the task except when the position error due to the trainee's mistake persists for a period of time. In that case, the haptic feedback guides the trainee to the right path. This situation happens in the experiments at $t \approx 5s, t \approx 10s$, and $t \approx 35s$.

In the next experiment, the task of following a 2D circular path is investigated. Remarkably, a 2D path requires the involvements of all three joints of the haptic device in the operation. Thus, the effectiveness of the proposed approach in the presence of nonlinear dynamics is evaluated more thoroughly. A graphical interface is provided for each operator to observe her/his own hand position as well as the other operators' hand position with respect to the circular path. The exper-

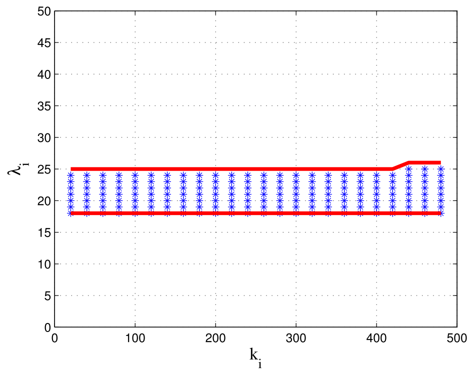

Fig. 4. The region satisfying stability condition.

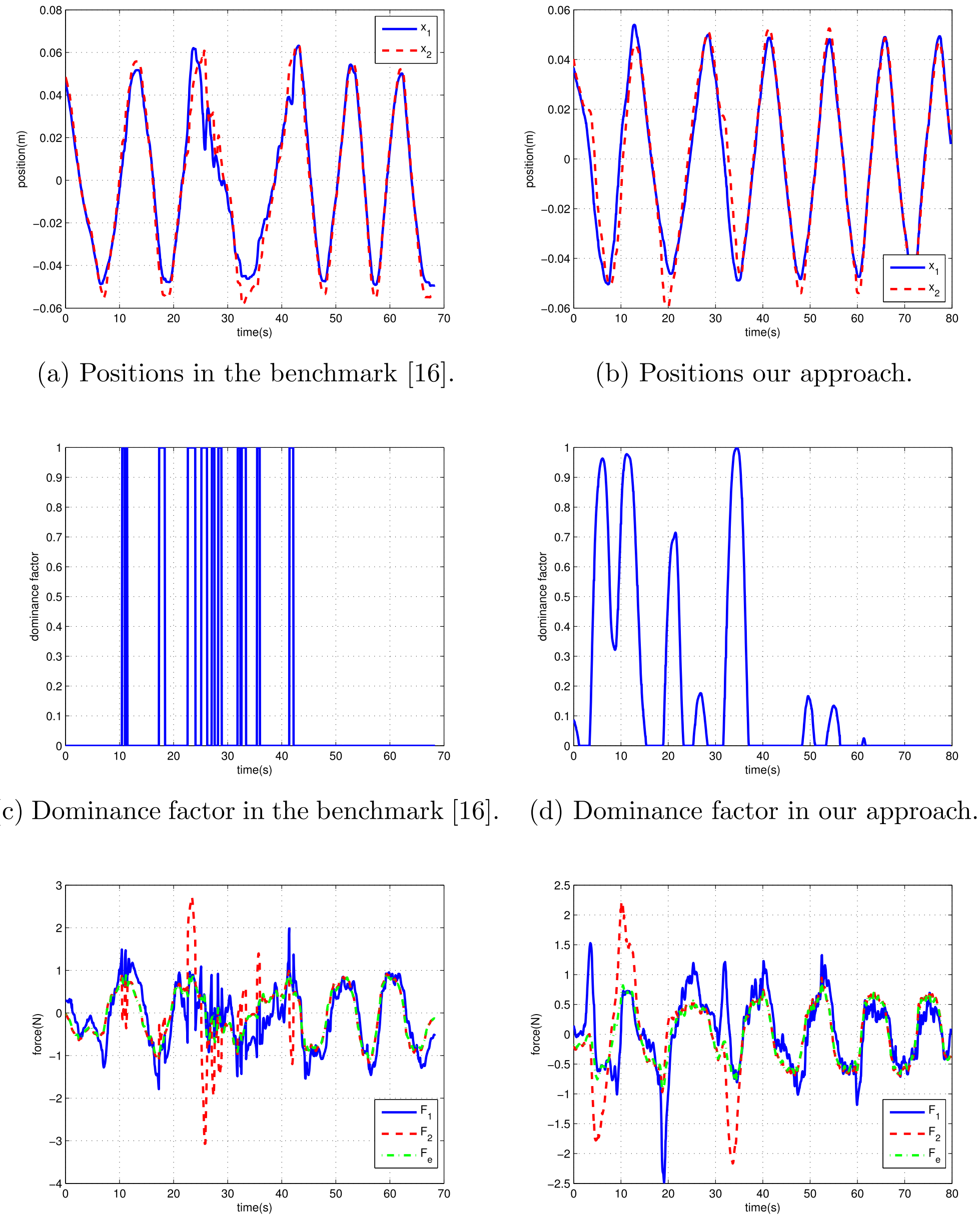

(a) Positions in the benchmark [16]. (b) Positions our approach.

(c) Dominance factor in the benchmark [16]. (d) Dominance factor in our approach.

(e) Forces in the benchmark [16]. (f) Forces in our approach.

Fig. 5. Experimental results in x direction.

imental results of this case are depicted in Fig. 6. The position variables in x direction and y direction of Cartesian coordinate are shown in Fig. 6a and Fig. 6b, respectively. Besides, the dominance factor is depicted in Fig. 6c and the force signals in x direction is shown in Fig. 6d. In addition, the position signals in xy plane are shown in Fig. 7. The results show that from $t = 0$ s to $t \approx 5$ s the trainee performs the task with negligible error with respect to the trainer. In this period, the position error is negligible and the task authority is given to the trainee. Afterwards, at the time $t \approx 5$ s the trainee is requested to deliberately perform wrong movements and generate position error to assess the behavior of the haptic system in correcting the trainee's mistakes. It can be seen that after this time, the dominance factor is unity for a few seconds and the task authority is given to the trainer. The haptic control structure tries to reduce the position error, but the trainee again performs wrong movements on purpose and the position error becomes considerable. Thus, the task authority is again given to the trainer until the trainee's task performance becomes satisfactory on $t \approx 22$ s to $t \approx 37$ s. Then, the trainee again performs wrong movements for a few seconds and the corrective feedback from the trainer is applied again to correct trainee's position. Next, after $t \approx 42$ s until the end of experiment the trainee performs task with small error such that his/her task performance becomes suitable and the task authority is given to the trainee. The position results show that during this time period the trainee performs the task with small amount of error with respect to the trainer. The force signals also shows that the force of environment in the majority of time periods matches the trainee's force and the trainee freely experience the task. However, when the position error due to the trainee's mistake persists for a period of time, those forces are do not match anymore and the haptic feedback is applied to guide the trainee to the right path.

7. Conclusions

This paper presents a robust control scheme with online authority adjustment for a dual user haptic system. In order to adjust task dominance, the position error between the trainer and the trainee in a sliding window is calculated as the task performance. Then, the magnitude of calculated task performance determines if and to what extent the corrective force feedback from the trainer to the trainee is necessary. The position tracking is ensures through a robust control structure and the stability of the closed loop system is analyzed using the ISS methodology and the small gain theorem. Experimental results

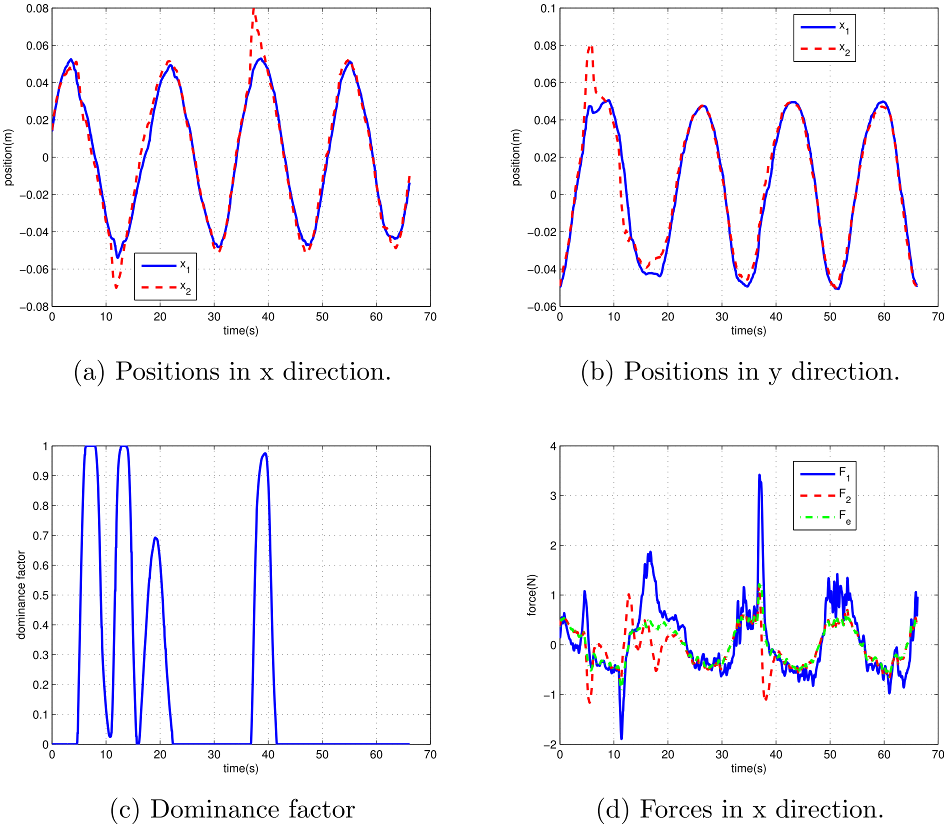

(a) Positions in x direction. (b) Positions in y direction.

(c) Dominance factor (d) Forces in x direction.

Fig. 6. Experimental results in xy plane.

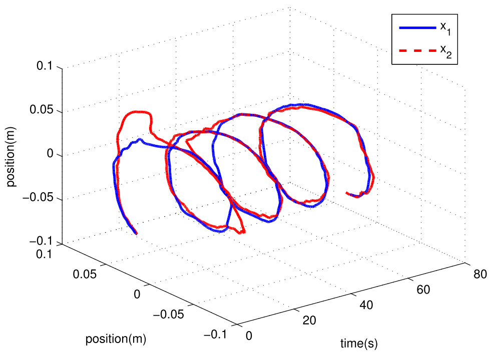

Fig. 7. The positions of haptic consoles in xy plane.

show the effectiveness of the proposed control approach. The next step is to determine other criteria to measure task performance of the trainee and combine them with the proposed control structure.

Acknowledgments

This work was supported in part by the National Institute for Medical Research Development (NIMAD) under Grant No. 942314.

Appendix A. Kinematics and dynamics of geomagic touch

The kinematics and dynamics equations of the Geomagic Touch haptic device is presented here. First, the position of the end effector is expressed as

$$x = -(l_1\cos(q_2) + l_2\sin(q_3))\sin(q_1)y = l_1\sin(q_2) - l_2\cos(q_3) + y_{\text{off}}z = (l_1\cos(q_2) + l_2\sin(q_3))\cos(q_1) - z_{\text{off}} \quad \text{(A.1)}$$

where the value of kinematic parameters l_1, l_2, y_{off}, and z_{off} are presented in Table A.1. Using (A.1), the Jacobian matrix of the haptic device can be calculated as

$$J = \begin{bmatrix} J_{11} & J_{12} & J_{13} \\ J_{21} & J_{22} & J_{23} \\ J_{31} & J_{32} & J_{33} \end{bmatrix}$$

where

$$\begin{aligned}
J_{11} &= -(l_1\cos(q_2) + l_2\sin(q_3))\cos(q_1) \\
J_{12} &= l_1\sin(q_1)\sin(q_2) \\
J_{13} &= -l_2\cos(q_3)\sin(q_1) \\
J_{21} &= 0 \\
J_{22} &= l_1\cos(q_2) \\
J_{23} &= l_2\sin(q_3) \\
J_{31} &= -(l_1\cos(q_2) + l_2\sin(q_3))\sin(q_1) \\
J_{32} &= -l_1\sin(q_2)\cos(q_1) \\
J_{33} &= l_2\cos(q_3)\cos(q_1)
\end{aligned}$$

Furthermore, the inertia matrix of the robot can be presented as

$$M(q) = \begin{bmatrix} M_{11} & p_5\sin(q_2) & 0 \\ p_5\sin(q_2) & p_6 & M_{23} \\ 0 & M_{23} & p_7 \end{bmatrix}$$

where

$$\begin{aligned}
M_{11} &= p_1 + p_2\cos(2q_2) + p_3\cos(2q_3) + p_4\cos(q_2)\sin(q_3) \\
M_{23} &= -0.5p_4\sin(q_2 - q_3).
\end{aligned}$$

In addition, the matrix $C(q,\dot{q})$ is given as

$$C(q,\dot{q}) = \begin{bmatrix} C_{11} & C_{12} & C_{13} \\ C_{21} & 0 & C_{23} \\ C_{31} & C_{32} & 0 \end{bmatrix}$$

Table A.1
The nominal values of the kinematic and dynamic parameters of Geomagic Touch haptic device.

Parameter	Value	Parameter	Value
l_1	133.35×10^{-3}	p_4	2.766×10^{-3}
l_2	133.35×10^{-3}	p_5	0.308×10^{-3}
z_{off}	168.35×10^{-3}	p_6	2.526×10^{-3}
y_{off}	23.35×10^{-3}	p_7	0.652×10^{-3}
p_1	1.798×10^{-3}	p_8	507.5×10^{-3}
p_2	0.864×10^{-3}	p_9	102.2×10^{-3}
p_3	0.486×10^{-3}	p_{10}	294.2×10^{-3}

where

$$\begin{aligned}
C_{11} = & -p2\dot{q}_2\sin(2q_2) - 0.5p4\dot{q}_2\sin(q_2)\sin(q_3) \\
& -p3\dot{q}_3\sin(2q_3) + 0.5p4\dot{q}_3\cos(q_2)\cos(q_3) \\
C_{12} = & \; p5\dot{q}_2\cos(q_2) - 0.5p4\dot{q}_1\sin(q_2)\sin(q_3) - p2\dot{q}_1\sin(2q_2) \\
C_{13} = & -p3\dot{q}_1\sin(2q_3) + 0.5p4\dot{q}_1\cos(q_2)\cos(q_3) \\
C_{21} = & \; p2\dot{q}_1\sin(2q_2) + 0.5p4\dot{q}_1\sin(q_2)\sin(q_3) \\
C_{23} = & \; 0.5p4\dot{q}_3\cos(q_2 - q_3) \\
C_{31} = & \; p3\dot{q}_1\sin(2q_3) + 0.5p4\dot{q}_1\cos(q_2)\cos(q_3) \\
C_{32} = & -0.5p4\dot{q}_2\cos(q_2 - q_3)
\end{aligned}$$

Finally, the vector $G(q)$ is expressed as

$$G(q) = \begin{bmatrix} 0 \\ p_8\cos(q_2) + p_{10}(q_2 - 0.5\pi) \\ p_9\sin(q_3) \end{bmatrix}. \tag{A.2}$$

The nominal values of the dynamic parameters are presented in Table A.1. Then, following some straightforward mathematical manipulation, the above dynamic system can be presented in the form of (2) with the parameter vector $\theta = [p_1 \quad p_2 \quad p_3 \quad p_4 \quad p_5 \quad p_6 \quad p_7 \quad p_8 \quad p_9 \quad p_{10}]^T$ and the regressor matrix as

$$Y = \begin{bmatrix} \ddot{q}_1 & y_{12} & y_{13} & y_{14} & y_{15} & 0 & 0 & 0 & 0 & 0 \\ 0 & y_{22} & 0 & y_{24} & y_{25} & \ddot{q}_2 & 0 & y_{28} & 0 & q_2 - 0.5pi \\ 0 & 0 & y_{33} & y_{34} & 0 & 0 & \ddot{q}_3 & 0 & y_{39} & 0 \end{bmatrix}$$

where

$$\begin{aligned}
y_{12} = & \; \ddot{q}_1\cos(2q_2) - 2\dot{q}_1\dot{q}_2\sin(2q_2) \\
y_{13} = & \; \ddot{q}_1\cos(2q_3) - 2\dot{q}_1\dot{q}_3\sin(2q_3) \\
y_{14} = & \; \ddot{q}_1\cos(q_2)\sin(q_3) - \dot{q}_1\dot{q}_2\sin(q_2)\sin(q_3) + \dot{q}_1\dot{q}_3\cos(q_2)\cos(q_3) \\
y_{15} = & \; \ddot{q}_2\sin(q_2) + \dot{q}_2\dot{q}_2\cos(q_2) \\
y_{22} = & \; \dot{q}_1\dot{q}_1\sin(2q_2) \\
y_{24} = & \; 0.5\,v1\dot{q}_1\sin(q_2)\sin(q_3) + 0.5\,v3\dot{q}_3\cos(q_2 - q_3) - 0.5a3\sin(q_2 - q_3) \\
y_{25} = & \; \ddot{q}_1\sin(q_2) \\
y_{28} = & \; \cos(q_2) \\
y_{33} = & \; \dot{q}_1\dot{q}_1\sin(2q_3) \\
y_{34} = & -0.5\dot{q}_2\dot{q}_2\cos(q_2 - q_3) + 0.5\dot{q}_1\dot{q}_1\cos(q_2)\cos(q_3) \\
y_{39} = & \; \sin(q_3)
\end{aligned}$$

References

[1] T. Do, T. Tjahjowidodo, M. Lau, S. Phee, Nonlinear friction modelling and compensation control of hysteresis phenomena for a pair of tendon-sheath actuated surgical robots, Mech. Syst. Sig. Process. 60 (2015) 770–784.
[2] M. Motaharifar, H.A. Talebi, F. Abdollahi, A. Afshar, Nonlinear adaptive output-feedback controller design for guidance of flexible needles, IEEE/ASME Trans. Mechatronics 20 (4) (2015) 1912–1919.
[3] D.O. Uribe, J. Schoukens, R. Stroop, Improved tactile resonance sensor for robotic assisted surgery, Mech. Syst. Sig. Process. 99 (2018) 600–610.
[4] I. Sharifi, H.A. Talebi, M. Motaharifar, A framework for simultaneous training and therapy in multilateral tele-rehabilitation, Comput. Electr. Eng. 56 (2016) 700–714.
[5] T. Endo, A. Kusakabe, Y. Kazama, H. Kawasaki, Haptic interface for displaying softness at multiple fingers: combining a side-faced-type multifingered haptic interface robot and improved softness-display devices, IEEE/ASME Trans. Mechatronics 21 (5) (2016) 2343–2351.
[6] J.B. Jonas, S. Rabethge, H.-J. Bender, Computer-assisted training system for pars plana vitrectomy, Acta Ophthalmol. Scand. 81 (6) (2003) 600–604.
[7] C. Basdogan, S. De, J. Kim, M. Muniyandi, H. Kim, M.A. Srinivasan, Haptics in minimally invasive surgical simulation and training, IEEE Comput. Graphics Appl. 24 (2) (2004) 56–64.
[8] J. Guo, S. Guo, T. Tamiya, H. Hirata, H. Ishihara, A virtual reality-based method of decreasing transmission time of visual feedback for a tele-operative robotic catheter operating system, Int. J. Med. Rob. Comput. Assist. Surg. 12 (1) (2016) 32–45.
[9] P. Agand, M. Motaharifar, H.D. Taghirad, Decentralized robust control for teleoperated needle insertion with uncertainty and communication delay, Mechatronics 46 (2017) 46–59.
[10] S. Ganjefar, S. Rezaei, F. Hashemzadeh, Position and force tracking in nonlinear teleoperation systems with sandwich linearity in actuators and time-varying delay, Mech. Syst. Sig. Process. 86 (2017) 308–324.
[11] S. Moghimi, S. Sirouspour, P. Malysz, Haptic-enabled collaborative training with generalized force and position mappings, in: Symp. Haptic Interfaces Virtual Environ. Teleoperator Syst., 2008, pp. 287–294.
[12] S.S. Nudehi, R. Mukherjee, M. Ghodoussi, A shared-control approach to haptic interface design for minimally invasive telesurgical training, IEEE Trans. Control Syst. Technol. 13 (4) (2005) 588–592.
[13] B. Khademian, K. Hashtrudi-Zaad, Dual-user teleoperation systems: new multilateral shared control architecture and kinesthetic performance measures, IEEE/ASME Trans. Mechatronics 17 (5) (2012) 895–906.

[14] F. Hashemzadeh, M. Sharifi, M. Tavakoli, Nonlinear trilateral teleoperation stability analysis subjected to time-varying delays, Control Eng. Pract. 56 (2016) 123–135.
[15] M. Motaharifar, A. Bataleblu, H. Taghirad, Adaptive control of dual user teleoperation with time delay and dynamic uncertainty, Iranian Conf. Electr. Eng. (2016) 1318–1323.
[16] F. Liu, A. Lelevé, D. Eberard, T. Redarce, A dual-user teleoperation system with online authority adjustment for haptic training, Annual Int. Conf. IEEE Eng. Medicine Biology Society (2015) 1168–1171.
[17] M. Shahbazi, S.F. Atashzar, H.A. Talebi, R.V. Patel, An expertise-oriented training framework for robotics-assisted surgery, Proc. IEEE Int. Conf. Rob. Autom. (2014) 5902–5907.
[18] M. Shahbazi, H.A. Talebi, R.V. Patel, Networked dual-user teleoperation with time-varying authority adjustment: A wave variable approach, Proc. IEEE/ASME Int. Conf. Adv. Intel. Mechatron. (2014) 415–420.
[19] Y. Hu, W. Gu, H. Zhang, H. Chen, Adaptive robust triple-step control for compensating cogging torque and model uncertainty in a dc motor, IEEE Trans. Syst., Man, Cybern.: Syst.
[20] H. Zhang, Y. Shi, J. Wang, H. Chen, A new delay-compensation scheme for networked control systems in controller area networks, IEEE Trans. Ind. Electron. 65 (9) (2018) 7239–7247.
[21] S. Khalilpour, R. Khorrambakht, H. Taghirad, P. Cardou, Robust cascade control of a deployable cable-driven robot, Mech. Syst. Sig. Process. 127 (2019) 513–530.
[22] X. Shao, J. Liu, H. Wang, Robust back-stepping output feedback trajectory tracking for quadrotors via extended state observer and sigmoid tracking differentiator, Mech. Syst. Sig. Process. 104 (2018) 631–647.
[23] M.W. Spong, M. Vidyasagar, Robot Dynamics and Control, John Wiley & Sons, 2008.
[24] C.C. de Wit, B. Siciliano, G. Bastin, Theory of Robot Control, Springer Science & Business Media, 2012.
[25] K. Razi, K. Hashtrudi-Zaad, Analysis of coupled stability in multilateral dual-user teleoperation systems, IEEE Trans. Rob. 30 (3) (2014) 631–641.
[26] A. Jafari, M. Nabeel, J.-H. Ryu, The input-to-state stable (iss) approach for stabilizing haptic interaction with virtual environments, IEEE Trans. Rob.
[27] H.K. Khalil, Nonlinear Systems, Prentice Hall, New Jewsey, 2002.
[28] H.L. Royden, P. Fitzpatrick, Real Analysis, fourth ed., Prentice Hall, Boston, MA, 2010.
[29] I.G. Polushin, A. Tayebi, H.J. Marquez, Control schemes for stable teleoperation with communication delay based on ios small gain theorem, Automatica 42 (6) (2006) 905–915.
[30] I. Polushin, H. Marquez, Stabilization of bilaterally controlled teleoperators with communication delay: an iss approach, Int. J. Control 76 (8) (2003) 858–870.
[31] B. Khademian, J. Apkarian, K. Hashtrudi-Zaad, Assessment of environmental effects on collaborative haptic guidance, Presence: Teleoperators Virtual Environ. 20 (3) (2011) 191–206.